Inorg. Chem. **2004**, *43*, 3543–3549

Structure of the Hydrated and Dimethyl Sulfoxide Solvated Rubidium Ions in Solution

Paola D'Angelo[†] and Ingmar Persson*[,‡]

Dipartimento di Chimica, Università di Roma "La Sapienza", Piazzale Aldo Moro 5, I-00185 Roma, Italy, and Department of Chemistry, Swedish University of Agricultural Sciences, P.O. Box 7015, SE-750 07 Uppsala, Sweden

Received November 4, 2003

The structure of the hydrated and the dimethyl sulfoxide solvated rubidium ions in solution has been determined by means of large-angle X-ray scattering (LAXS) and extended X-ray absorption fine structure (EXAFS) studies. The models of the hydrated and dimethyl sulfoxide solvated rubidium ions fitting the experimental data best are square antiprisms with Rb–O bond distances of 2.98(2) and 2.98(3) Å, respectively. The EXAFS data show a significant asymmetry in the Rb–O bond distance distribution with C_3 values of 0.0076 and 0.015 Å^3, respectively. No second hydration sphere is observed around the hydrated rubidium ion. The dimethyl sulfoxide solvated rubidium ion displays a Rb–O–S bond angle of ca. 130°, which is typical for a medium hard electron acceptor such as rubidium.

Introduction

The alkali-metal ions, except the small lithium ion, are very weakly solvated,[1−6] and crystallize normally without coordinated solvent molecules.[7,8] In this study an attempt to determine the structure of the hydrated and dimethyl sulfoxide solvated rubidium ions in solution by means of large-angle X-ray scattering (LAXS) and extended X-ray absorption fine structure (EXAFS) methods is made. To construct models for evaluating the weak and possibly irregular coordination around the hydrated rubidium ion in aqueous solution in the current structure study, a literature search was performed. A very large number of crystal structures of rubidium compounds are reported in the literature where rubidium is surrounded by oxygen atoms.[7,8] In most compounds no well-defined coordination figure around the rubidium ion is present, and the Rb−O distances vary within a very wide range. The Rb−O bond distances in the rubidium compounds and complexes are in most cases in the range 2.7−3.2 Å.[7,8] However, in some compounds symmetric coordination figures around rubidium are present, e.g., a square antiprism and a dodecahedron. Shannon has given the ionic radius of the rubidium ion as 1.52, 1.61, 1.66, and 1.72 Å in six-, eight-, ten-, and twelve-coordination, respectively.[9] An EXAFS study on the acetonitrile solvated rubidium ion is so far the only reported structure on a rubidium ion in solution.[10] The Rb−N bond distance was determined to be 2.95(2) Å, with a coordination number of about seven.

The aim of the present study is to get a better idea of the structure of the hydrated and dimethyl sulfoxide solvated rubidium ions in solution, which may serve as a basic model for the solvated potassium and cesium ions in solution. A combination of LAXS and EXAFS techniques is used to detect the Rb−O bond distances to the weakly bound solvent molecules as accurately as possible.[11]

Experimental Section

Chemicals. Anhydrous rubidium fluoride, RbF (Merck), rubidium iodide, RbI (Aldrich), and rubidium trifluoromethanesulfonate, $RbCF_3SO_3$ (Aldrich), were used as purchased, and

* Author to whom correspondence should be addressed. E-mail: ingmar.persson@kemi.slu.se.
[†] Università di Roma "La Sapienza".
[‡] Swedish University of Agricultural Sciences.

(1) Rosseinsky, D. R. *Chem. Rev.* **1965**, *65*, 467 and references therein.
(2) Morris, D. F. C. *Struct. Bonding (Berlin)* **1968**, *4*, 63.
(3) Ahrland, S. In *The Chemistry of Non-Aqueous Solvents*; Lagowski, J. J., Ed.; Academic Press: New York, 1978; Vol. VA, Chapter 1 and references therein.
(4) Marcus, Y. *Pure Appl. Chem.* **1983**, *55*, 977.
(5) Marcus, Y. *Pure Appl. Chem.* **1985**, *57*, 1103.
(6) Inerowicz, H. D.; Li, W.; Persson, I. *J. Chem. Soc., Faraday Trans.* **1994**, *90*, 2223.
(7) Allen, F. H.; Bellard, S.; Brice, M. D.; Cartwright, B. A.; Doubleday, A.; Higgs, H.; Hummelink, T.; Hummelink-Peters, G. G.; Kennard, O.; Motherwell, W. D. S.; Rodgers, J. R.; Watson, D. G. The Cambridge Crystallographic Data Centre: computer-based search, retrieval, analysis and display of information. *Acta Crystallogr., Sect. B* **1979**, *35*, 2331 and references therein.
(8) Inorganic Crystal Structure Data Base, National Institute of Standards and Technology, Fachinformationszentrum, Karlsruhe, Release 03/1.
(9) Shannon, R. D. *Acta Crystallogr., Sect A* **1976**, *32*, 751.
(10) D'Angelo, P.; Pavel, N. V. *J. Chem Phys.* **1999**, *111*, 5107.

10.1021/ic030310t CCC: $27.50
Published on Web 05/07/2004

Table 1. Concentrations (mol·dm^{-3}), Densities (ρ/g·cm^{-3}), and Linear Absorption Coefficients (μ/cm^{-1}) of the Aqueous and Dimethyl Sulfoxide (Me_2SO) Solutions Used in the Large-Angle X-ray Scattering (L) and EXAFS (E) Measurements

sample	[Rb^+]	[X^-]	[solvent]	ρ	μ	method
RbF in water	3.01	3.01	52.60	1.260	24.40	L
RbI in water	1.51	1.51	50.13	1.227	19.91	L
$RbCF_3SO_3$ in water	1.00	1.00	52.50			E
$RbC_6H_2(NO_2)_3O$ in Me_2SO	1.31	1.31	12.02	1.342	14.49	L
RbI in Me_2SO	0.80	0.80	12.60			E

rubidium picrate, $RbOC_6H_2(NO_2)_3$, was prepared as described elsewhere.[12] Dimethyl sulfoxide (Merck) was freshly distilled over calcium hydride (Fluka) under reduced pressure.

Sample Preparation. The aqueous rubidium fluoride, iodide, and trifluoromethanesulfonate solutions and the dimethyl sulfoxide solutions of rubidium picrate and iodide were prepared by dissolving weighed amounts of the salt in the respective solvent. The composition of the studied samples is given in Table 1.

EXAFS Analysis. The Rb K-edge X-ray absorption data were collected in transmission mode at beam line 4-1, Stanford Synchrotron Radiation Laboratory (SSRL), under dedicated conditions; SSRL operates at 3.0 GeV and a maximum current of 100 mA. A Si[220] double-crystal monochromator was detuned to 50% of the maximum intensity at the end of the scans to discard higher order harmonics. The solutions were kept in cells with 6.3 μm X-ray polypropylene foil windows and a 1 mm Teflon spacer. The energy calibration of the X-ray absorption spectra was performed by simultaneously recording the spectrum of a rubidium chloride sample, and assigning the first K-edge inflection point to 15200 eV.[13] Three scans of each sample were recorded, energy calibrated, and averaged.

The EXAFS data analysis was performed with the GNXAS code using previously developed and widely applied methods.[14,15] In the GNXAS approach the interpretation of the experimental data is based on the decomposition of the EXAFS $\chi(k)$ signal (defined as the oscillation with respect to the atomic background cross-section normalized to the corresponding K-edge channel cross-section[16]) into a summation over n-body distribution functions $\gamma^{(n)}$ calculated by means of the multiple-scattering (MS) theory. Each signal has been calculated in the muffin-tin approximation using the Hedin−Lundqvist energy-dependent exchange and correlation potential model, which includes inelastic loss effects.[15]

X-ray absorption spectra at the Rb K-edge are well-known to be affected to a high degree by anomalies associated with the opening of multielectron excitation channels.[17,18] In the case of solutions, due to the weakness of the structural signal, the use of a proper atomic background model is an essential prerequisite to perform a reliable EXAFS data analysis. To this end double-electron excitations can be accounted for by modeling the atomic background as the sum of a smooth polynomial spline plus step-shaped functions

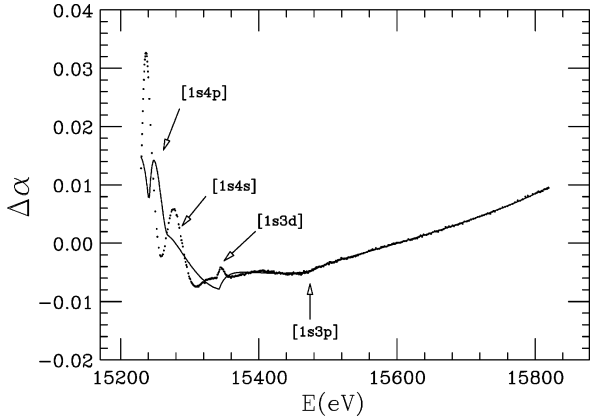

Figure 1. XAS spectrum of the aqueous solution of rubidium trifluoromethanesulfonate after subtraction of a linear component (dotted line) and the adopted atomic background function (sold line). Arrows mark the calculated energy thresholds for the double-excitation processes involving the 1s and 4p, 4s, 3d, and 3p electrons, respectively.

as described in ref 14. Each function depends on three parameters, which represent the edge position relative to the single-hole state E_d, the width ΔE, and the jump H of the double-electron channel contribution.

The spectrum of the aqueous rubidium trifluoromethanesulfonate solution and the atomic background used to isolate the structural contribution are shown in Figure 1. The ordinate $\Delta\alpha$ corresponds to the absorption excess, which is calculated by subtracting an average decay from the absorption spectrum fitted in the EXAFS region, and normalized to the K-edge discontinuity. Arrows in Figure 1 indicate the energy positions of the double-electron transitions associated with the 4p, 4s, 3d, and 3p electrons, obtained from HF theoretical calculations.[18] A very similar background model has been used in the analysis of the dimethyl sulfoxide solution. Note that the atomic background used to extract the $\chi(k)$ signal closely reassembles the X-ray absorption spectrum of rubidium vapor, thus enforcing the reliability of the present analysis.[18] Attempts to extract EXAFS data from EXAFSPAK and WinXAS program packages did unfortunately fail, and it was only by the approach used in the GNXAS program, described above, that a reasonable $\chi(k)$ function was obtained.

Several EXAFS investigations on electrolyte solutions have shown that a correct description of the first solvation sphere has to account for asymmetry in the distribution of the ion−solvent distances. Therefore, the Rb−O first coordination shells have been modeled with Γ-like distribution functions which depend on four parameters, namely, the coordination number N, the average distance R, the mean-square variation σ^2, and the skewness β. Note that β is related to the third cumulant C_3 through the relation $C_3 = \sigma^3\beta$.

X-ray absorption spectroscopy is endowed with the unique capability of providing quantitative information on the three-body distribution functions in disordered systems. In the case of the dimethyl sulfoxide solution, the $\gamma^{(3)}$ signal associated with the Rb−O−S three-body distribution has been calculated by means of the

(11) Persson, I.; Sandström, M.; Yokoyama, H.; Chaudhry, M. *Z. Naturforsch.* **1995**, *50a*, 21.
(12) Willard, H. H.; Smith, G. F. *J. Am. Chem. Soc.* **1923**, *45*, 286.
(13) Thompson, A.; Attwood, D.; Gullikson, E.; Howells, M.; Kim, K.-J.; Kirz, J.; Kortright, J.; Lindau, I.; Pianatta, P.; Robinson, A.; Scofield, J.; Underwood, J.; Vaughan, D.; Williams, G.; Winick, H. *X-ray Data Booklet*; LBNL/PUB-490 Rev. 2; Lawrence Berkeley National Laboratory: Berkeley, CA, 2001.
(14) Filipponi, A.; Di Cicco, A. *Phys. Rev. B* **1995**, *52*, 15135.
(15) Filipponi, A.; Di Cicco, A.; Natoli, C. R. *Phys. Rev. B* **1995**, *52*, 15122.
(16) Sayers, D. E.; Bunker, B. A. In *X-ray absorption: Principles, Applications, Techniques of EXAFS, SEXAFS and XANES*; Koningsberger, D. C., Prins, R., Eds.; Wiley-Interscience: New York, 1988; Chapter 6.
(17) D'Angelo, P.; Di Nola, A.; Giglio, E.; Mangoni, M.; Pavel, N. *J. Phys. Chem.* **1995**, *99*, 5471.
(18) Kodre, A.; Arcon, I.; Padenik Gomilsek, J. Preseren, R.; Frahm, R. *J. Phys. B: At. Mol. Opt. Phys.* **2002**, *35*, 3497.

Table 2. Model Fitting of LAXS and EXAFS Data[a]

system	interaction	N	d	σ^2	C_3	S_o^2	method
RbI in water, 1.51 mol·dm^{-3}	Rb−O	8	2.990(8)	0.0120(6)			L
	I···O	6	3.584(6)	0.0102(5)			
	O···O	2	2.817(5)	0.0124(8)			
RbF in water, 3.01 mol·dm^{-3}	Rb−O	8	2.961(6)	0.0124(6)			L
	F···O	6	2.66(2)	0.011(3)			
	O···O	2	2.884(12)	0.0125(7)			
$RbCF_3SO_3$ in water, 1.00 mol·dm^{-3}	Rb−O	8.0(5)	2.98(4)	0.049(3)	0.0076(5)	0.98	E
	Rb···H	16	3.75(10)	0.18(4)	0.07(3)		
$RbOC_6H_2(N\ O_2)_3$ in Me_2SO, 1.31 mol·dm^{-3}	Rb−O	8	2.964(8)	0.0154(6)			L
	Rb···S	8	4.070(6)	0.034(2)			
RbI in Me_2SO, 0.80 mol·dm^{-3}	Rb−O	7.9(5)	3.01(4)	0.060(6)	0.015(8)	0.98	E
	S−O	7.9(5)	1.52(2)	0.005(2)			
	Rb···S[b]	7.9(5)	4.18(5)	0.055(8)			

[a] Mean bond distances, d/Å, Debye−Waller factor coefficients, σ^2/Å^2, number of distances, N, asymmetry parameters (or third cumulants), C_3/Å^3, and amplitude reduction factors, S_o^2, in the EXAFS studies, of the solvated rubidium ion in solution as determined by EXAFS (E) and LAXS (L) at room temperature. [b] The Rb−O−S angle has been refined to 137(4)°.

GNXAS program, and a thorough description of the theoretical framework used in the MS data analysis has been reported elsewhere.[14] The only structural parameters associated with the Rb−O−S $\gamma^{(3)}$ contribution are the Rb−O and S−O bond distances and the Rb−O−S bond angle. The Rb···S two-body signal is calculated starting from the same structural parameters.

The standard deviations given for the refined parameters in Table 2 are obtained from k^3-weighted least-squares refinements of the EXAFS function $\chi(k)$, and do not include systematic errors of the measurements. These statistical error estimates provide a measure of the precision of the results and allow reasonable comparisons, e.g., of the significance of relative shifts in the distances. However, the variations in the refined parameters, including the shift in the E_o value (for which $k = 0$), using different models and data ranges, indicate that the absolute accuracy of the distances given for the separate complexes is within ±0.01−0.02 Å for well-defined interactions. The "standard deviations" given in the text have been increased accordingly to include estimated additional effects of systematic errors.

Large-Angle X-ray Scattering. The scattering from the free surface of aqueous solutions of rubidium fluoride and iodide was measured by means of a large-angle $\theta-\theta$ diffractometer, using Mo Kα radiation, $\lambda = 0.7107$ Å. The solutions were contained in an open Teflon cup with an airtight radiation shielding with beryllium windows. The scattered radiation was monochromatized in a focusing LiF crystal monochromator, and the intensity was measured at discrete points in the range $1° < \theta < 65°$; the scattering angle is 2θ. The scattering variable s is defined as $s = 4\pi\lambda^{-1} \sin\theta$. A total of 100000 counts were accumulated at each preset angle, and the entire angular range was scanned twice, which corresponds to a statistical error of about 0.3%. The divergence of the primary X-ray beam was limited by 1°, 1/4°, or 1/12° slits for different θ regions, with overlapping data for scaling purposes. The technical description of the experimental setup and the most important equations in the data treatment have been presented elsewhere.[19] All data treatment was carried out by means of the KURVLR program.[20] The experimental intensities were normalized to a stoichiometric unit of volume containing one rubidium atom, using the scattering factors f for neutral atoms, including corrections for anomalous dispersion,[21] $\Delta f'$ and $\Delta f''$, and values for Compton scattering.[22] Least-squares refinements of the model parameters were carried out by means of the STEPLR program,[23] where the expression $U = \sum[si_{exptl}(s) - si_{calcd}(s)]^2$ is minimized, where U is the error square sum and $i(s)$ reduced intensity. The refinement of the model parameters was made for data in the high s region where the intensity contribution from the diffuse and long-range distances can be neglected.[24] To obtain a better alignment of the intensity function before the refinements, a Fourier back-transformation procedure was used to correct the $i_{exptl}(s)$ functions by removing spurious nonphysical peaks below 1.2 Å in the experimental radial distribution function (RDF).[25] The errors given in Table 2 of the parameters obtained from the LAXS method include only the statistical errors, while the errors given throughout the text also include the estimated systematic errors.

Strengths of the EXAFS and LAXS Techniques. The structure determination of the rubidium ion in aqueous and dimethyl sulfoxide solution shows nicely that the EXAFS and LAXS techniques are complementary. The EXAFS method has its strength in the ability to separate short well-defined distances and describe asymmetry in bond distance distribution, which is not possible with the LAXS method, due to the much larger momentum range available for the former one.[26] The intensity functions of the EXAFS and LAXS methods show that the amplitude is much faster damped in the former, which means that long distances with relatively large distance distribution are not seen in EXAFS, while they can be clearly seen in LAXS.[26,27]

Results and Discussion

Hydrated Rubidium Ion. The radial distribution function of an aqueous solution of 1.5 mol·dm^{-3} rubidium iodide shows two distinct peaks, at 2.9 and 3.6 Å, below 6 Å; see Figure 2. The first peak corresponds mainly to two interactions, the Rb−O bond distance in the hydrated rubidium ion and the O−(H)···O distances within the aqueous bulk, and the second peak to I···(H)−O distances of the hydrated

(19) Stålhandske, C. M. V.; Persson, I.; Sandström, M.; Kamienska-Piotrowicz, E. *Inorg. Chem.* **1997**, *36*, 3174.
(20) Johansson, G.; Sandström, M. *Chem Scr.* **1973**, *4*, 195.
(21) *International Tables for X-Ray Crystallography*; Wilson, A. J. C., Ed.; Kluwer Academic Publishers: Dordrecht, The Netherlands, 1995; Vol. C; Kynoch Press: Birmingham, U.K., 1974; Vol. 4.
(22) Cromer, D. T. *J. Chem. Phys.* **1969**, *50*, 4857.
(23) Molund, M.; Persson, I. *Chem. Scr.* **1985**, *25*, 197.
(24) Sandström, M.; Persson, I.; Ahrland, S. *Acta Chem. Scand., Ser. A* **1978**, *32*, 607.
(25) Levy, H. A.; Danford, M. D.; Narten, A. H. *Data Collection and Evaluation with an X-Ray Diffractometer Designed for the Study of Liquid Structure*; Report ORNL-3960; Oak Ridge National Laboratory; Oak Ridge, TN, 1966.
(26) Persson, I.; Sandström, M.; Yokoyama, H.; Chaudhry, M. *Z. Naturforsch., B: Chem. Sci.* **1995**, *50*, 21.
(27) Persson, I.; Persson, P.; Sandström, M.; Ullström, A.-S. *J. Chem. Soc., Dalton Trans.* **2002**, 1256.

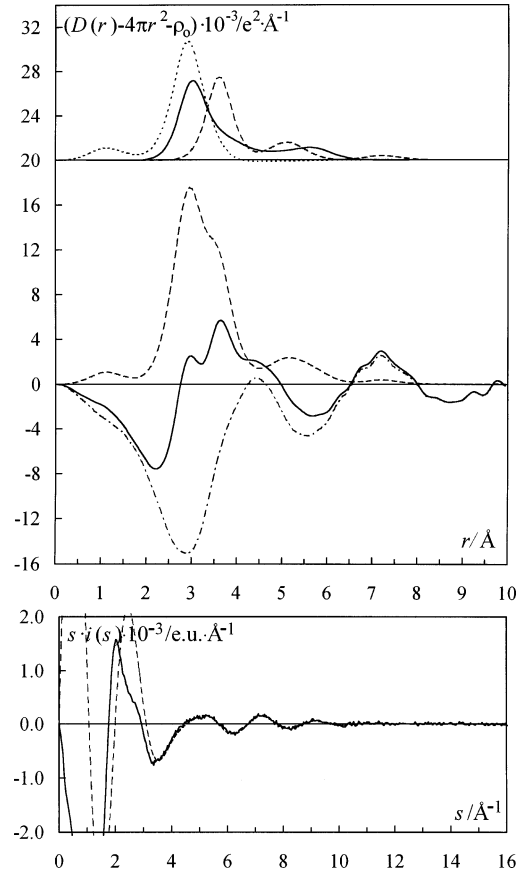

Figure 2. LAXS. (Top) Individual peak shapes for all contributing species in the 1.50 mol·dm^{-3} aqueous solution of rubidium iodide (offset +20): Rb−O interactions in the first hydration shell (solid line), the hydrated iodide ion (dashed line), and O···O distances in aqueous bulk (dotted line). (Middle) Experimental $D(r) - 4\pi r^2\rho_o$ (solid line), model (dashed line), and difference (dashed−dotted line). (Bottom) Reduced LAXS intensity functions $si(s)$ (solid line) and model $si_{calcd}(s)$ (dashed line).

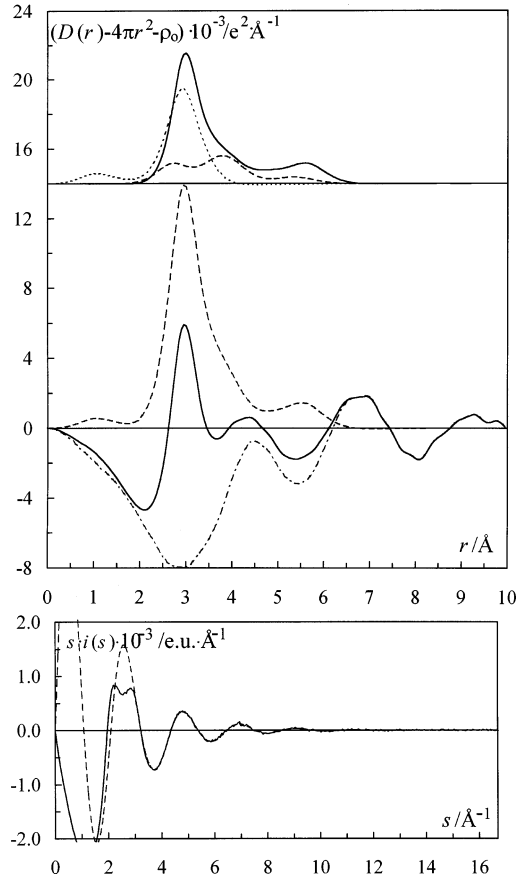

Figure 3. LAXS. (Top) Individual peak shapes for all contributing species in the 3.01 mol·dm^{-3} aqueous solution of rubidium fluoride (offset +14): Rb−O interactions in the first hydration shell (solid line), the hydrated fluoride ion (dashed line), and O···O distances in aqueous bulk (dotted line). (Middle) Experimental $D(r) - 4\pi r^2\rho_o$ (solid line), model (dashed line), and difference (dashed−dotted line). (Bottom) Reduced LAXS intensity functions $si(s)$ (solid line) and model $si_{calcd}(s)$ (dashed line).

iodide ion. Refinements of the $Rb(OH_2)_8$ and $I(\cdots(H)-O)_6$ clusters, and of the O···(H)−O interactions in the aqueous bulk resulted in Rb−O, I···(H)−O, and O···(H)−O distances of 2.99(1), 3.58(2), and 2.82(2) Å, respectively. The O···O interactions within the square antiprismatic $Rb(OH_2)_8$ cluster are seen as a weak shoulder at ca. 4.0 Å, while the expected weak interaction at 5.55 Å is hardly seen in the RDF (cf. Figure 2). The I···(H)−O distance in the hydrated iodide ion, assumed to be surrounded by six water molecules, is in close agreement with previous results.[28,29] The coordination number of the hydrated halide ions is six for all halides in aqueous solution, as indicated by the same difference in the X···(H)−O distances in aqueous solution as the difference in ionic radii for the six-coordinated halide ions given by Shannon.[9] Broad peaks often remain at ca. 4 Å in the LAXS difference function for aqueous solutions of large and weakly hydrated ions (cf. Figures 1 and 2, Figures 1−6 in ref 30,[30] Figure 2 in ref 31,[31] and Figure 1 in ref 32[32]). This probably reflects a distribution of O−(H)···O distances shorter than normal in the water structure, caused by a partial breakdown of the hydrogen bonding due to the presence of the large structure-breaking ions poorly fitting into the bulk structure. A detailed theoretical modeling to explain these experimental observations is still lacking. The structural parameters are summarized in Table 2. The fit of the experimental intensity data and the RDF with the individual contributions are given in Figure 2.

The radial distribution function of an aqueous solution of 3.0 mol·dm^{-3} rubidium fluoride shows below 6 Å one distinct peak at 2.9 Å; see Figure 3. This peak corresponds to several interactions, the Rb−O bond distance in the hydrated rubidium ion, the F···(H)−O distance of the hydrated fluoride ion, reported to be 2.60−2.69 Å in aqueous solution,[28,29] and the O−(H)···O distances within the aqueous bulk occurring at about 2.89 Å in pure water.[29] Refinements of the $Rb(OH_2)_8$ and $F(\cdots(H)-O)_6$ clusters and of O···(H)−O interactions in the aqueous bulk resulted in Rb−O, F···(H)−O, and O···(H)−O distances of 2.96(2), 2.66(4), and 2.88(4) Å, respectively. The F···(H)−O distance in the hydrated fluoride ion, surrounded by six water molecules, is in close agreement with previous results.[28,29] The O···(H)−O distance

(28) Ohtaki, H.; Radnai, T. *Chem. Rev.* **1993**, *93*, 1157 and references therein.
(29) Johansson, G. *Adv. Inorg. Chem.* **1992**, *39*, 159 and references therein.
(30) Lyxell, D.-G.; Pettersson, L.; Persson, I. *Inorg. Chem.* **2001**, *40*, 584.
(31) Jalilehvand, F.; Spångberg, D.; Lindqvist-Reis, P.; Hermansson, K.; Persson, I.; Sandström, M. *J. Am. Chem. Soc.* **2001**, *123*, 431.
(32) Persson, I.; Jalilehvand, F.; Sandström, M. *Inorg. Chem.* **2001**, *40*, 584.

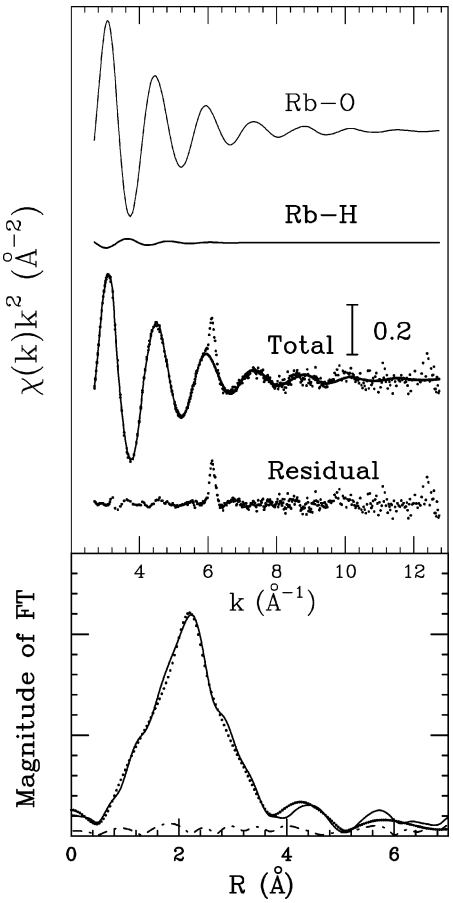

Figure 4. EXAFS. (Top) Fit of the aqueous solution of rubidium trifluoromethanesulfonate. From the top to the bottom of the panel the following curves are reported: Rb−O and Rb−H first shell two-body signals, total theoretical signal (solid line) compared with the experimental spectrum (dotted line) and residual. (Bottom) Non-phase-shift-corrected Fourier transforms of EXAFS experimental data (dotted line), of the theoretical signal (solid line), and of the residual curve (dashed−dotted line) calculated over the range $2.8 < k < 12.7$ Å^{-1}.

within the aqueous bulk, 2.88 Å, is very close the value previously found in pure water,[29] showing that the rubidium and fluoride ions perturb the aqueous bulk only to a small degree. The O···O interactions within the square antiprismatic $Rb(OH_2)_8$ and the octahedral $F(\cdots(H)-O)_6$ clusters are seen as a weak shoulder at ca. 3.9 Å; see Figure 3. The lack of strong contributions around 4.5 Å in both aqueous solutions of rubidium studied strongly indicates that no well-defined second hydration sphere is present around the hydrated rubidium ion; the second hydration spheres are seen very clearly in hydrated di- and trivalent metal ions, as well as in the hydrated silver(I) and thallium(I) ions.[28,29,33,34] The structural parameters are summarized in Table 2. The fit of the experimental intensity data and the RDF with the individual contributions are given in Figure 3.

The results of the EXAFS data analysis performed on the 1.0 mol·dm^{-3} rubidium trifluoromethanesulfonate aqueous solution are shown in Figure 4. In the upper panel we report the Rb−O and Rb−H two-body theoretical signals, their sum compared with the experimental spectrum, and the resulting residual. As expected, the dominant contribution to the total EXAFS curve is given by the Rb−O first shell signal, but the Rb−H signal is clearly detectable, and its amplitude is above the experimental noise of the spectrum. Nevertheless, due to the weakness of the Rb−H contribution, the hydrogen structural parameters obtained from the minimization are affected by large systematic errors (see Table 2). The sharp peak at about 6.1 Å^{-1} is associated with the opening of the 1s3d double-excitation channels, and it does not have its origin in a structural contribution.[17] For this reason the experimental points in a range of about 20 eV around this peak have been excluded from the fitting procedure. The magnitudes of the Fourier transforms (FTs), non-phase-shift-corrected, of the experimental, theoretical, and residual signals are shown in the lower panel of Figure 4. Least-squares refinement of the Rb−O first hydration shell resulted in an asymmetric distribution of the water molecules around the rubidium ion, with a median bond distance of 2.98(4) Å. Refined values of the full set of structural parameters are listed in Table 2. The energy onset E_d, the width ΔE, and the jump H of the double-electron excitation edges have been found equal to those reported in ref 17, while the zero position of the theoretical scale was 1.0(5) eV above the first inflection point of the spectrum. It is important to stress that S_o^2, which accounts for the reduced overlap between the passive electrons in the ground-state and the excited-state relaxed configurations, is strongly correlated with the first shell coordination number. This makes it difficult to obtain reliable information on the coordination geometry around the photoabsorber, when multielectron excitation effects are not properly accounted for in the EXAFS data analysis. On the other hand, when a proper background model is used, S_o^2 is expected to be close to 1.0,[35] and this result has been previously found for the Rb^+ ion.[17]

Dimethyl Sulfoxide Solvated Rubidium Ion. The radial distribution function of a 1.31 mol·dm^{-3} dimethyl sulfoxide solution of rubidium picrate shows three peaks, a double peak at 1.5−1.9 Å corresponding to intramolecular bond distances in the solvent and the picrate ion, a peak at 2.75 Å containing large contributions from intramolecular distances in the solvent and the picrate ion as well as Rb−O bond distances in the dimethyl sulfoxide solvated rubidium ion, and a peak at 4.2 Å corresponding to Rb···S distances in the dimethyl sulfoxide solvated rubidium ion; see Figure 5. The coordination number of the dimethyl sulfoxide solvated rubidium ion is close to eight, which is in accordance with the observation in aqueous solution, see above, and the ionic radius given by Shannon.[9] The large broad peaks at ca. 5.5 and 9 Å are typical for dimethyl sulfoxide solutions and correspond to intermolecular distances.[36] The structural parameters are summarized in Table 2. The Rb−O−S bond angle is 127.4(8)°, which is typical for a medium hard electron acceptor.[37] The

(33) Yamaguchi, T.; Johansson, G.; Holmberg, B.; Maeda, M.; Ohtaki, H. *Acta Chem. Scand., Ser. A* **1984**, *38*, 437.
(34) Persson, I.; Jalilehvand, F.; Sandström, M. *Inorg. Chem.* **2002**, *41*, 192.
(35) D'Angelo P.; Di Cicco, A.; Filipponi, A.; Pavel, N. V. *Phys. Rev. A* **1995**, *47*, 2005.
(36) Ahrland, S.; Hansson, E.; Iverfeldt, Å.; Persson, I. *Acta Chem. Scand., Ser. A* **1981**, *35*, 275.

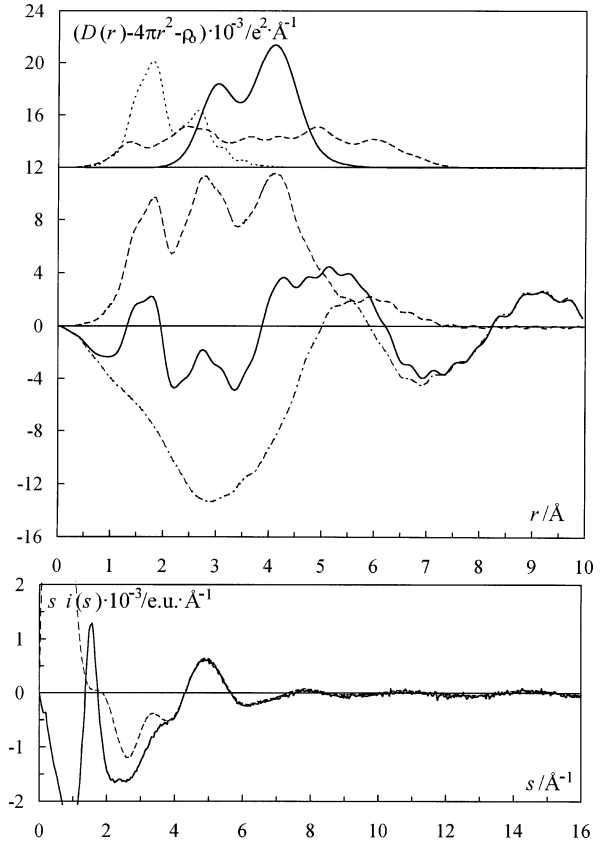

Figure 5. LAXS. (Top) Individual peak shapes for all contributing species in the 1.31 mol·dm^{-3} dimethyl sulfoxide solution of rubidium picrate (offset +12): Rb−O and Rb···S distances in the dimethyl sulfoxide solvated rubidium ion (solid line), the picrate ion (dashed line), and the solvent dimethyl sulfoxide (dotted line). (Middle) Experimental $D(r) - 4\pi r^2\rho_o$ (solid line), model (dashed line), and difference (dashed−dotted line). (Bottom) Reduced LAXS intensity functions $si(s)$ (solid line) and model $si_{calcd}(s)$ (dashed line).

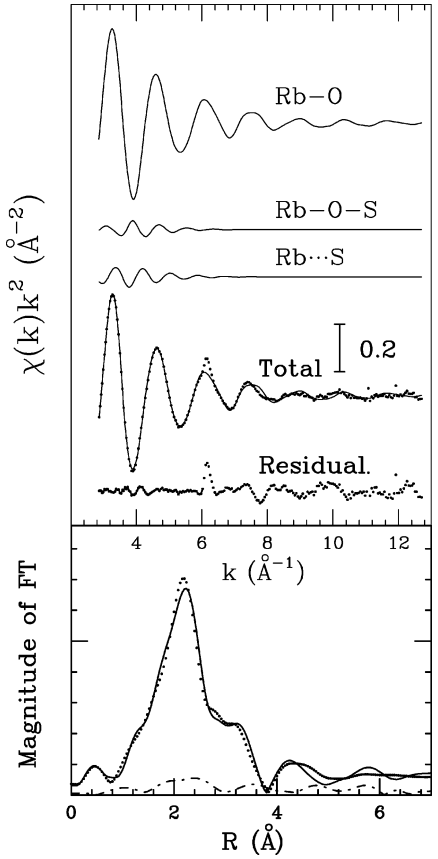

Figure 6. EXAFS. (Top) Fit of the dimethyl sulfoxide solution of rubidium iodide. From the top to the bottom of the panel the following curves are reported: Rb−O two-body signal, Rb−O−S three-body signal, Rb···S two-body signal, total theoretical signal (solid line) compared with the experimental spectrum (dotted line) and residual. (Bottom) Non-phase-shift-corrected Fourier transforms of EXAFS experimental data (dotted line), of the theoretical signal (solid line), and of the residual curve (dashed−dotted line) calculated over the range $2.9 < k < 12.7$ Å^{-1}.

fit of the experimental intensity data and the RDF with the individual contributions are given in Figure 5.

The results of the EXAFS data analysis performed on the 0.8 mol·dm^{-3} rubidium iodide/dimethyl sulfoxide solution are shown in Figure 6. The first three curves from the top correspond to the Rb−O $\gamma^{(2)}$, Rb−O−S $\gamma^{(3)}$, and Rb···S $\gamma^{(2)}$ contributions. The reminder of the figure shows the total theoretical signal compared with the experimental spectrum and the resulting residual. Also in this case the experimental points around 6.1 Å^{-1} have been excluded from the fitting procedure. The magnitudes of the FTs, non-phase-shift-corrected, of the experimental, theoretical, and residual signals are shown in the lower panel of Figure 6. The structural parameters obtained from the minimization are listed in Table 2. The Rb−O−S angle is 132(4)° with a bond angle variance of 4.5°, in agreement with the LAXS determination. According to the EXAFS results the Rb···S distance is 4.18(5) Å with a Debye−Waller factor of 0.055(8) Å^2, while the zero position of the theoretical scale is 1.5(5) eV above the first inflection point of the spectrum.

The distances obtained from the LAXS and EXAFS studies are in very good agreement, while the Debye−Waller factor coefficients, σ^2, are larger from the EXAFS data than from the LAXS data. A possible reason can be that the EXAFS technique is less sensitive to long and more diffuse interaction than the LAXS technique.[26] In the previous study on the hydration and solvation of the thallium(I) ion, the same trend was observed with larger σ^2 values from the EXAFS data,[34] while for strong interactions the difference is negligible.

Conclusions

The weakly hydrated and dimethyl sulfoxide solvated rubidium ions both seem to be surrounded by ca. eight solvent molecules, probably in square antiprismatic fashion, at a mean bond distance of 2.98(2) and 2.98(3) Å, respectively. These results and those for the previously reported acetonitrile solvated rubidium ion, d(Rb−N) = 2.95 Å,[10] show that the rubidium has a fairly well-defined solvation shell in both water and nonaqueous solvents with a reasonable high dipole moment, and that ca. eight solvent molecules are clustered around the rubidium ion in the solvents studied. The Rb−O bond distribution is clearly asymmetric with C_3 values of 0.0076 and 0.015 Å^3 for the hydrate and dimethyl sulfoxide solvate, respectively. Using the atomic radius of water oxygen, 1.34 Å,[38] the ionic radius of the eight-

(37) Calligaris, M.; Carugo, O. *Coord. Chem. Rev.* **1996**, *153*, 83 and references therein.

coordinated rubidium ion is ca. 1.64 Å, which is in good agreement with the value proposed by Shannon, 1.61 Å.[9]

Acknowledgment. We gratefully acknowledge the Italian National Research Council and the Ministry for the University and the Scientific and Technological Research (MURST) (P.D.) and the Swedish Research Council (I.P.) for financial support. Portions of this research were carried out at the Stanford Synchrotron Radiation Laboratory, a national user facility operated by Stanford University on behalf of the U.S. Department of Energy, Office of Basic Energy Sciences. The SSRL Structural Molecular Biology Program is supported by the Department of Energy, Office of Biological and Environmental Research, and by the National Institutes of Health, National Center for Research Resources, Biomedical Technology Program.

IC030310T

(38) Beattie, J. K.; Best, S. P.; Skelton, B. W.; White, A. H. *J. Chem. Soc., Dalton Trans.* **1981**, 2105.